Transactions of the Materials Research Society of Japan 28 [3] 867-870 (2003)

Magnetic and Transport Properties in Fe and Oxide-coated Fe Cluster Assemblies

Dong-Liang Peng*, Takehiko Hihara and Kenji Sumiyama
Department of Materials Science and Engineering, Nagoya Institute of Technology,
Gokiso-cho, Showa-ku, Nagoya 466-8555, Japan
*Fax: 81-52-735-5309; E-mail: pengdl@mse.nitech.ac.jp

Size-monodispersed Fe and oxide-coated Fe cluster assemblies were prepared by a plasma-gas-condensation-type cluster beam deposition apparatus. A large hysteresis loop shift (namely a unidirectional exchange anisotropy) induced by field cooling was observed for the oxide-coated Fe cluster assemblies. This should originate from a strong exchange coupling between Fe core and Fe-oxide shell layer, although the oxide layers were identified to be two ferrimagnetic phases (Fe_3O_4 or r-Fe_2O_3). We have also further studied electrical resistivity and magnetoresistance effect in these Fe cluster assemblies between 5 and 300 K. The magnetoresistance values depend on temperature and surface oxidization degree of the clusters. Magnetic field dependence of magnetoresistance exhibits no saturation tendency in fields up to 5 T even at low temperatures, which disagrees with magnetization curves. Such a high-field non-saturation behavior and the unidirectional exchange anisotropy mentioned above are believed to result from the disordered surface spin structure of the small Fe-oxide crystallites.
Key words: Fe cluster, oxide-coated Fe cluster, magnetism, magnetoresistance, plasma-gas-condensation

1. INTRODUCTION

With the rapid development of magnetic recording media, the memory unit size is going down to smaller than 100 nm. Superparamagnetism is a serious problem because the magnetization direction is eliminated by thermal fluctuation. In particular, the super-paramagnetism and the coercivity of single-domain particle systems often depends on the size and size distribution of magnetic particles. In order to optimize the magnetic properties of particle- or cluster-assembled materials, control of particle size distribution is also of immense importance. We have recently developed the plasma-gas- condensation (PGC) type cluster beam deposition apparatus [1], which is a vapor-phase synthesis of clusters. Since metal vapors are produced by sputtering of a target material, a wide variety of elements can serve as source materials [2]. Using this system, we have obtained monodispersed transition metal clusters (Cr [1,3], Co [4] and Fe [5]) with the mean cluster diameters d from a few to a few tens of nanometers and the standard deviation less than 10% of d.

In this paper we deal with magnetic and transport properties in the size-monodispersed Fe and oxide-coated Fe cluster assemblies. We also study magnetoresistance effect and the relationship between the magnetoresistance (MR) ratio and the flow rate of oxygen gas (namely surface oxidization degree) in these monodispersed Fe and oxide-coated Fe cluster assemblies.

2. EXPERIMENTAL

The samples were prepared by the PGC-type cluster beam deposition apparatus, whose detail was described elsewhere [1,6]. We can control the cluster size by changing the flow rate of Ar gas, R_{Ar}, and the flow rate of He gas, R_{He}. For preparation of oxide-coated Fe cluster assemblies, we introduced oxygen gas through a nozzle set near the skimmer into the deposition chamber to form iron oxide shells covering the Fe clusters before depositing on the substrate. This process ensures that all Fe clusters are uniformly oxidized before the cluster assemblies are formed. For constant R_{Ar} or $R_{Ar} + R_{He}$, the gas pressure in the deposition chamber can be adjusted lower than 6×10^{-4} Torr by changing the flow rate of oxygen gas (R_{O2}). We used three kinds of substrates for the Fe cluster deposition: microgrid, which was covered by a carbon-coated colodion film and supported by a Cu grid, for transmission electron microscope (TEM) observations, quartz substrates for electrical conduction and magnetoresistance measurement, and polyimide films for magnetic measurement. The effective film thickness of deposited clusters, t_e, was estimated using a quartz crystal thickness monitor, which measures the weight of the deposited clusters. Magnetic and magnetoresistance measurement was performed using a superconducting quantum interference device magnetometer between 5 and 300 K with the maximum field of 50 kOe.

3. RESULTS AND DISCUSSION

3.1 Morphology and microstructural characterization

For oxide-coated Fe cluster assemblies, coexistence of bcc α-Fe and Fe_3O_4 or γ-Fe_2O_3 phases was confirmed by the electron diffraction patterns (not shown here). Figure 1(a) shows BF-TEM micrograph of the oxide-coated Fe cluster assemblies with d = 13 nm and the effective thickness $t_e \approx 2.5$ nm prepared at R_{O2} = 3 sccm. Almost all clusters are characterized with a strong contrast in their "core", but with a uniform gray contrast in their "shell". Figure 1(b) shows a high-resolution TEM micrograph of the core-shell cluster observed in the same aggregate. The lattice fringe 0.203 nm shown by two arrows in the core is

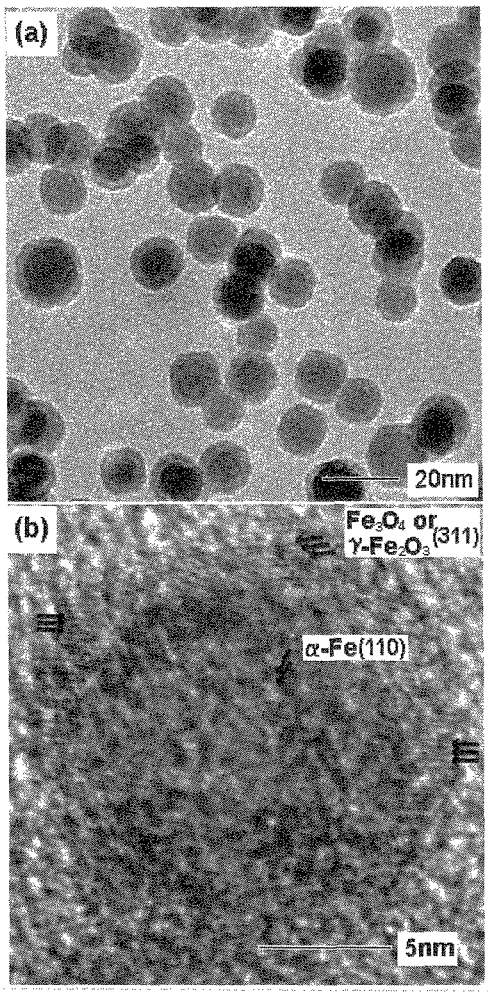

Fig. 1 (a) Bright-field TEM micrograph of the oxide-coated Fe clusters with d = 13 nm prepared on a carbon microgrid at the O_2 gas flow rate R_{O2} = 3 sccm. Almost all clusters show a core-shell structure. (b) High-resolution TEM micrograph of an oxide-coated Fe cluster, found in the same cluster sample.

attributable to the α-Fe phase while the lattice fringes 0.253 nm shown by three arrows in the shell to the {311} spacing of Fe_3O_4 or γ-Fe_2O_3 phase. These results also indicate that the oxide-coated Fe clusters were covered with the Fe_3O_4 or γ-Fe_2O_3 shells composed of very small crystallites (about grain size of 2nm).

3.2 Magnetic behaviors

Hysteresis loops were measured at 5 K after zero field cooling (ZFC) and field cooling (FC) the samples from 300 to 5 K in a magnetic field, H, of 20 kOe. The direction of H used to measure the loops was parallel to that of the cooling field. Figure 2 shows the ZFC and FC loops of the oxide-coated Fe cluster assemblies with d = 9 nm prepared at R_{O2} = 3 sccm. The large shift of the FC loop in comparison with the symmetric feature in the ZFC loop is detected. Coercivity H_c (in both ZFC and FC cases) and the loop shift increases with increasing R_{O2} (not shown here). These features confirm the presence of a unidirectional

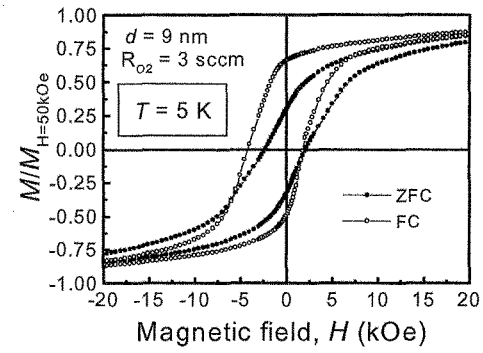

Fig. 2 Hysteresis loops of the zero-field-cooled (ZFC) and field-cooled (FC) oxide-coated Fe cluster assembly with d = 9 nm prepared at R_{O2} = 3 sccm.

exchange anisotropy [7]. Note that the unidirectional exchange anisotropy originates from the presence of an antiferromagnetic oxide layers covering the ferromagnetic clusters [7,8], although the oxide layers were identified to be two ferrimagnetic phases.

In order to further investigate the unidirectional exchange anisotropy, we measured the dependence of the exchange bias field H_{eb} on repeated magnetization reversals, namely the so-called training effect which is a diminution of H_{eb} upon the subsequent magnetization reversals [9]. Figure 3(a) shows typical results from the loops measured along the field-cooling direction at 5 K for the oxide-coated Fe cluster assembly with d = 9 nm and R_{O2} = 3 sccm. The successive loops do not

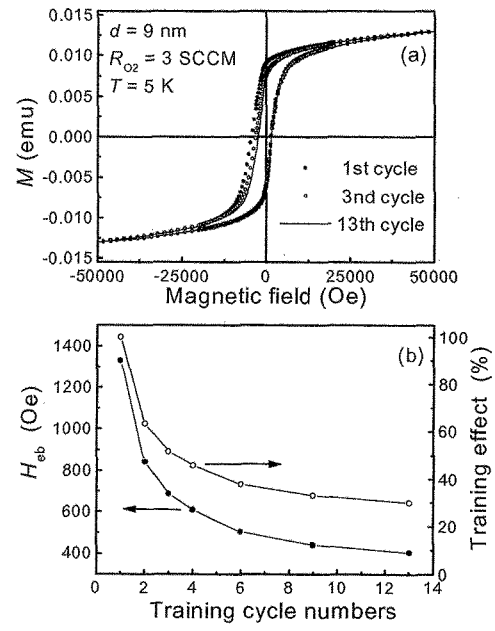

Fig. 3 (a) Successive hystersis loops measured at 5 K after cooling from 300 K in a field of +20000 Oe along the same direction; (b) H_{eb} and training effect as a function of the training cycle number for the oxide-coated Fe cluster assembly with d = 9 nm prepared at R_{O2} = 3 sccm.

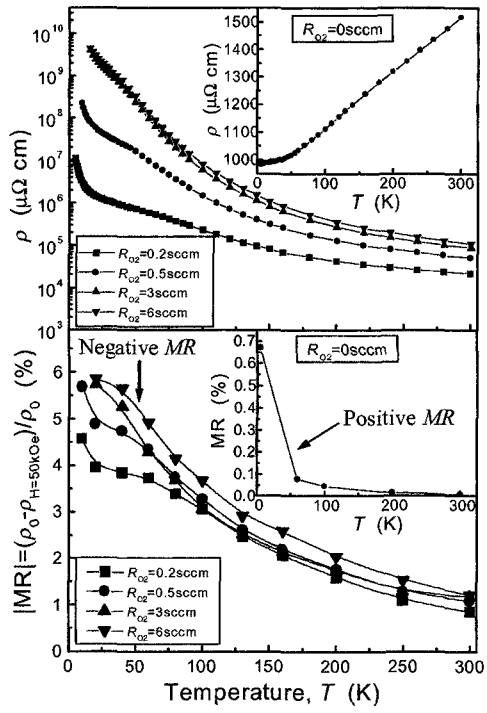

Fig. 4 Temperature dependence of (a) electrical resistivity ρ and (b) absolute value of the magnetoresistance ratio, $|MR|$, at H =50 kOe for the oxide-coated Fe cluster assemblies prepared at R_{O2} = 0, 0.2, 0.5, 3 and 6 sccm. The insets show the results for R_{O2} = 0 sccm.

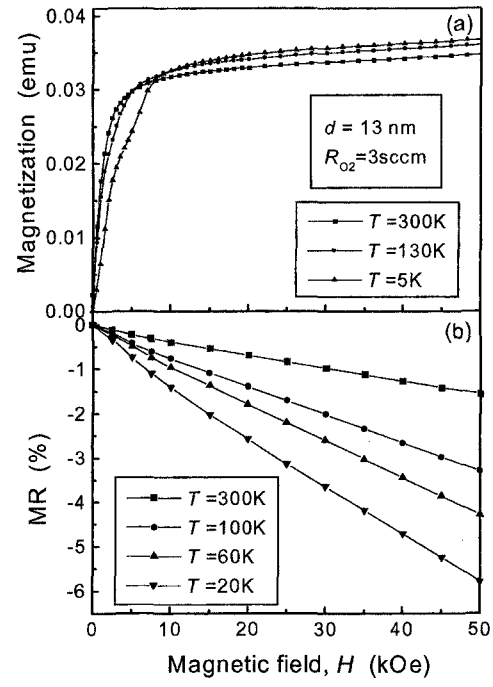

Fig. 5 Magnetic field dependence of (a) magnetization and (b) magnetoresistance ratio, $MR=(\rho_{H=50kOe}-\rho_0)/\rho_0$, at different temperatures for the oxide-coated Fe cluster assembly with d = 13 nm prepared at R_{O2} = 3 sccm..

coincide with each other and show a decrease in H_{eb}. Figure 3(b) shows the dependence of H_{eb} and the training effect on the training cycle number at 5 K. Here, we define the training effect as the fraction of the initial value which is lost after field cycling. The decrease of H_{eb} is remarkable with increasing the training cycle number and the training effect is decreased to about 30% after the 13th cycle.

3.3 Magnetoresistance effects

Figure 4(a) shows the temperature (T) dependence of the electrical resistivity, $\rho(T)$, for the oxide-coated Fe cluster assemblies with d = 13 nm prepared at R_{O2} = 0, 0.2, 0.5, 3 and 6 sccm. For R_{O2} = 0 sccm (see the inset of Fig. 4(a)), the sample shows ordinary metallic temperature dependence, characterized by the residual resistance at low temperatures and a linear increase with increasing T. For R_{O2} > 0.2 sccm, the temperature coefficient of resistivity (TCR) becomes negative. Moreover, the resistivity at low temperature is three to five orders of magnitude larger than that at room temperature and about 5-7 orders of magnitude larger than that of the sample prepared at R_{O2} = 0 sccm. Such an abrupt increase in the resistivity of the present cluster assemblies is attributable to the tunnel-type conduction between metallic Fe cores via Fe-oxide shell layers.

Figure 4(b) shows the temperature (T) dependence of high-field MR ratio, $[\rho_{H=50kOe}-\rho_0]/\rho_0$, for the oxide-coated Fe cluster assemblies with d = 13 nm prepared at R_{O2} = 0, 0.2, 0.5, 3 and 6 sccm. For R_{O2} = 0 sccm (see the inset of Fig. 4(b)), we have observed a small positive magnetoresistance effect, similar to the case of the multilayers [10-12] and Pd-C granular films [13], which has been ascribed to a weak localization effect. For R_{O2} > 0.2 sccm, large negative magnetoresistance effect was observed. With decreasing T, the absolute value of MR increases monotonically increases and reaches to about 6% at T = 20 K for R_{O2} = 6 sccm.

Figure 5 shows the magnetic field dependence of magnetization and MR ratio at different temperatures for the oxide-coated Fe cluster assemblies with d = 13 nm prepared at R_{O2} = 3 sccm. Clearly, the field-dependent feature of the MR effect which exhibits no saturation tendency disagrees with the magnetization curves (Fig.5(a)) which are of a saturation tendency in spite of gradual increase of magnetization for H > 10 kOe. In nanogranular alloys containing uncorrelated magnetic scatters such as superparamagnetic magnetic particles [14], the MR values should be proportional to M^2. Since magnetotunneling is an interface effect, the high-field non-saturation behavior for the present systems may result from spin disorder at the Fe-oxide grain surface [15]. Such a surface spin disorder has been experimentally discussed in ferrite nanoparticles [16] and small Fe oxide grains [17]. The antiferromagnetic superexchange interaction is disrupted at the surface of the ferrimagnetic oxide crystallites because of missing oxygen ions or presence of other impurity molecules. Such broken exchange bonds between surface spins lead to surface spin disorder, similar to a spin-glass state. According to such hypothesis of the spin-glass-like state in the

interfacial layers between the Fe core and Fe-oxide shell, the unidirectional exchange anisotropy and training effect observed at low temperature (Fig. 2 and 3) can also be explained reasonably. The repeated magnetization reserval at high fields makes the interfacial spins change to a new frozen spin state and decreases the initial net magnetization, causing a decrease of H_{eb} and H_c.

4. CONCLUSIONS

Using the PGC type cluster beam deposition technique, we have produced the monodispersed Fe cluster assemblies with a mean diameter of d = 7.3 – 16.3 nm. By surface oxidation process under low O_2 pressure (< 6×10^{-4} Torr), the monodispersed Fe cluster assemblies covered by the Fe_3O_4 or γ-Fe_2O_3 shells are also obtained. Large hysteresis loop shifts (namely exchange bias field H_{eb}) induced by field cooling was observed. The decrease of H_{eb} is remarkable with increasing the training cycle number and the training effect is decreased to about 30% after the 13th cycle. On the other hand, the Fe cluster assembly shows a small positive MR effect while the oxide-coated Fe cluster assemblies exhibit a large negative *GMR* effect which mainly results from a spin-dependent tunneling effect. Saturation behaviors in *M-H* and *MR-H* are remarkably different. High-field non-saturation feature in *MR* can be attributed to the disordered surface spin structure of the small Fe-oxide shell crystallites, which is also the predominant origin to the unidirectional exchange anisotropy and training effect at low temperature.

ACKNOWLEDGMENTS

This work has been supported by Core Research for Evolutional Science and Technology (CREST) of Japan Science and Technology Corporation (JST). One of the authors (D. L. Peng) appreciates the financial support from Japan Society for the Promotion of Science (JSPS).

References

[1] S. Yamamuro, K. Sumiyama, M. Sakurai, and K. Suzuki, *Supramol. Sci.*, **5**, 239-245 (1998).
[2] H. Haberland, M. Karrais, M. Mall and Y. Thurner, *J. Vac. Sci. Technol. A*, **10**, 3266-3271 (1992).
[3] S. Yamamuro, K. Sumiyama, and K. Suzuki, *J. Appl. Phys.*, **85**, 483-489 (1999).
[4] S. Yamamuro, K. Sumiyama, T. J. Konno, and K. Suzuki, *Mater. Trans., JIM* **40**, 1450-1455 (1999).
[5] D. L. Peng, K. Sumiyama, T. Hihara, and H. Morikawa, *J. Appl. Phys.*, **92**, 3075-3083 (2002).
[6] D. L. Peng, K. Sumiyama, T. Hihara, and T. J. Konno, *Scripta Mater.* **44**, 1471-1474 (2001).
[7] W. H. Meiklejohn and C. P. Bean, *Phys. Rev.*, **102**, 1413-1414 (1956); **105**, 904-913 (1957).
[8] B. D. Cullity, "Introduction to Magnetic Materials", Addison-Wesley, London(1972) pp. 422-425.
[9] M. Holdenried, B. Hackenbroich, and H. Micklitz, *J. Magn. Magn. Mater.*, **231**, 13-19 (2001).
[10] H. Sato, I. Sakamoto, and C. Fierz, *J. Phys.: Condens. Matter*, **3**, 9067-9078 (1991).
[11] C. Uher, R. Clarke, G. Zheng, and I. K. Schuller, *Phys. Rev. B*, **30**, 453-455 (1984).
[12] M. T. Perez and J. L. Vicent, *Phys. Rev. B*, **38**, 9503-9510 (1988).
[13] A. Carl, G. Dumpich, and D. Hallfarth, *Phys. Rev. B*, **39**, 915-922 (1989); *Phys. Rev. B*, **39**, 3015-3020 (1989); *Thin Solid Films*, **193/194**, 1065-1072 (1990).
[14] C. L. Chien, J. Q. Xiao and J. S. Jiang, *J. Appl. Phys.*, **73**, 5309-5314 (1993).
[15] L. Savini, E. Bonetti, L. Del Bianco, L. Pasquini, S. Signoretti, P. Allia, M. Coisson, J. Moya, V. Selvaggini, P. Tiberto and F. Vinai, *J. Appl. Phys.*, **91**, 8593-8595 (2002).
[16] R. H. Kodama, A. E. Berkowitz, E. J. McNiff, and S. Foner, *Phys. Rev. Lett.*, **77**, 394-397 (1996).
[17] L. Del Bianco, A. Hernando, M. Multigner, C. Prados, J. C. Sanchez-Lopez, A. Fernandez, C. F. Conde and A. Conde, *J. Appl. Phys.*, **84**, 2189-2192 (1998).

(Received December 20, 2002; Accepted March 1, 2003)